Desalination and Water Treatment
www.deswater.com
doi: 10.1080/19443994.2016.1179225

57 (2016) 28486–28495
December

Taylor & Francis
Taylor & Francis Group

Efficient removal of acid dye from aqueous solutions via adsorption using low-cost blast-furnace slag

Danhua Zhao*, Qinbaio Qiu, Yanni Wang, Mengru Huang, Yinghong Wu, Xiaojun Liu, Tao Jiang

Department of Chemistry, Guangdong University of Education, Guangzhou 510303, P.R. China, email: zhaodanhua@gdei.edu.cn (D. Zhao)

Received 28 August 2015; Accepted 10 April 2016

ABSTRACT

Acid Red 138 (AR138) and Acid Green 27 (AG27) were efficiently removed from aqueous solutions via adsorption using modified blast-furnace slag (MBFS). The surface of MBFS was investigated using scanning electron microscopy and Brunauer–Emmett–Teller method. The effects of operating parameters such as adsorbent dosage, pH, and temperature on the dye removal were studied. The pseudo-first-order, pseudo-second-order, and intraparticle diffusion models were used to describe the kinetics data. The equilibrium isotherms were analyzed using the Langmuir and Freundlich adsorption models. The experimental data fitted well to the pseudo-second-order kinetics model for AR138 and AG27. The Freundlich isotherm described the equilibrium data of acid dyes on MBFS better than the Langmuir isotherm. Furthermore, the thermodynamic parameters ($\Delta G_0 < 0$, $\Delta H_0 < 0$, and $\Delta S_0 < 0$) showed that the adsorption reactions of AR138 and AG27 onto MBFS were feasible, spontaneous, and exothermic under the investigated conditions. Thus, MBFS is an effective biosorbent for the removal of acid dyes.

Keywords: Slag; Modification; Acid dye; Adsorption

1. Introduction

Nowadays, the environmental impact of effluents from many industries including textile, leather, cosmetics, paper, printing, plastic, food, and pharmaceuticals has increased significantly. Dyes are one of the major constituents of effluents. Even small quantities of dyes can color large water bodies, thus not only affecting the esthetic merit, but also reduce light penetration and photosynthesis. Moreover, many dyes and their degradation products are harmful toward aquatic life and humans [1,2]. Therefore, colored effluents should be treated properly before they are discharged into water bodies [3,4].

Generally, dye-containing effluents are mainly treated by physical, chemical, biological, and acoustical, radiation, and electrical processes [5]. Moreover, many other physiochemical methods have been used for the removal of dyes, such as electrochemical treatment [6], advanced oxidation technology [7], and membrane filtration [8]. However, these methods are not efficient or economic [6–8]. Recently, adsorption techniques have attracted interest because of simple operation, cost-effectiveness, readily available adsorbents, and removal efficiency [4,9]. Activated carbon is the most common adsorbent for dye removal by adsorption,

*Corresponding author.

but the high cost of activated carbon limits its use in practical applications [9,10]. Many studies are being carried out to find inexpensive, commercially available materials to replace activated carbon. Renewable and inexpensive adsorbent precursors from industrial and agricultural byproducts have been used for the removal of dyes from wastewater [11–18].

Blast-furnace slag is the byproduct of steel industries in a large scale. The slag in long-term stock not only occupies a large amount of land, but also causes environmental pollution, becoming more and more evident and severe. Thus, a suitable method or technique is highly desired to utilize low-cost slag materials. Currently, this is mainly used as a filler or in the production of slag cement [19–21]. The sorption characteristics of slag, however, have not been fully investigated, except for some reports on the removal of heavy metals [22–24], phosphate [25,26], and ammonium and organic pollutants [26] from wastewater. Because of porous nature with a large surface area and a wide particle distribution, slag has great potential for the removal of dyes from colored waters. A few studies on the removal of dyes from wastewater have been reported [5,27–29]. In this study, a combination of HCl and NaCl was used as the impregnant for the chemical activation of blast-furnace slag waste, and this treated material was used as the adsorbent to remove two acid dyes, AG27 and AR138. The equilibrium, isotherm models, and kinetics data of the biosorption studies were analyzed to understand the biosorption mechanism of AG27 and AR138 onto modified blast-furnace slag (MBFS).

2. Materials and methods

All the chemicals were purchased from Sigma-Aldrich (Germany) or Sinopharm Chemical Reagent Co. (Shanghai, China) and used as received without further purification. Doubly distilled water was used throughout the experiments.

Two acid dyes (Table 1), Acid Red 138 (AR138) and Acid Green 27 (AG27), were selected as the adsorbate for investigating the adsorption performance of MBFS. The initial pH of the solution was adjusted using 0.1 M NaOH or 0.1 M HCl solution. The pH was measured using a pH meter (3109-01, Thermo Orion, USA).

2.1. Preparation of adsorbent

The slag was obtained from Shanxi province, China, washed repeatedly with water to remove the adhering dirt and water-soluble impurities, dried at 100°C for 3 h, and crushed. The dried slag was ground using a universal high-speed smashing machine (FW80, Beijing Yongguangming Medical Equipment Factory, China) to powder and passed through China Standard Sieves (<63 μm). The MBFS was prepared by mixing 30 g of raw slag with 90 mL of a mixture of 3.5 M HCl and 0.1 M NaCl solution. The mixture was stirred at 500 rpm at room temperature for 2 h. The liquid was decanted, and the wet slag was dried at 100°C for 3 h. The obtained material, i.e. MBFS, was ground repeatedly. Finally, The MBFS was stored in an airtight brown glass container and used for analysis and adsorption experiments.

2.2. Physicochemical properties and characterization of slag and MBFS

The morphological characteristics of the raw and modified slag were obtained using a scanning electron microscope (SEM) (Model S-4800, Hitachi, Japan). The main chemical compositions of the samples were measured (Table 2) using an X-ray fluorescence spectrometer (PW2424, Philips, Netherlands). The specific surface areas of the samples were determined from the N_2 sorption isotherms at −196°C by applying the Brunauer–Emmett–Teller (BET) method using a surface area analyzer (ASAP2020, Micromeritics, USA), The pore-size distribution of the samples was calculated by the Barrett–Joyner–Halenda (BJH) method.

2.3. Adsorption experiments

The batch adsorption experiments were carried out at room temperature (25°C). The stock solutions of AR138 and AG27 (600 mg/L) were prepared and suitably diluted to the required initial concentrations. The isotherm experiments were carried out in 50-mL flasks containing 20 mL of the dye solution and 0.10 g of MBFS. The mixtures were stirred in dark for 60 min. The final equilibrium concentrations of the dyes were measured spectrophotometrically after the centrifugation. The adsorption experiments were conducted in a batch system. The effects of some parameters such as pH (4.0–10.0), time (0–120 min), temperature (15–55°C), and adsorbent dosage (0.02–0.12 g/L) on the adsorption of AG27 onto MBFS were evaluated using a known amount of the adsorbent and 10 mL of the dye solution of a known concentration in a series of capped 10-mL flasks. The initial pH of the dye solution was previously adjusted using 0.1 M NaOH or 0.1 M HCl solution. The mixture was shaken using a water bath and constant temperature oscillator (SHY-2A, China) at 160 rpm at 25°C for 2 h. After each adsorption process, the residual dye solution was obtained by filtration, and the

Table 1
Structure, molar mass, and the maximum absorption wavelength (λ_{max}) of three dyes

Name	Structure	Molar mass (g/mol)	λ_{max} (nm)
Acid Red 138 CAS no. 15792-43-5	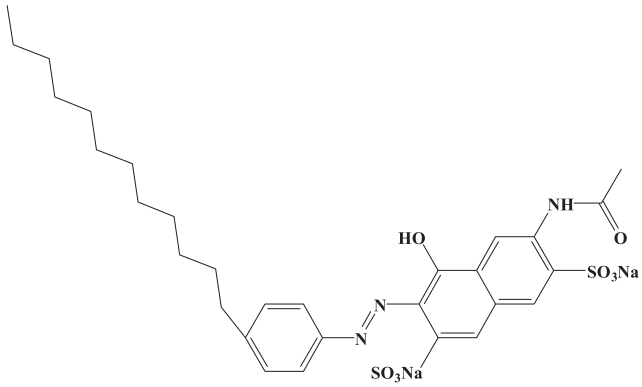	677.74	570
Acid Green 27 CAS no. 6408-57-7	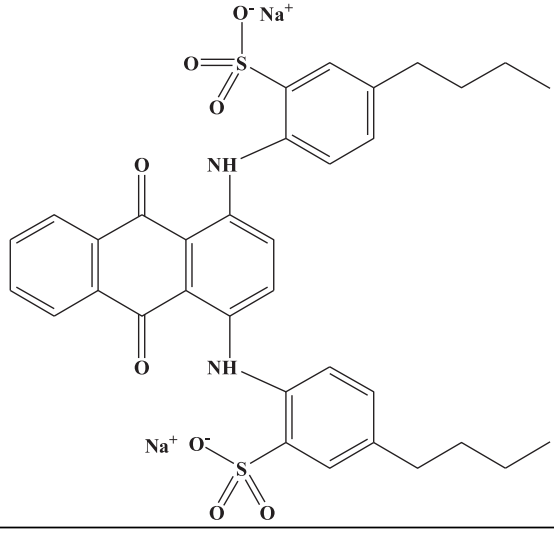	706.74	646

Table 2
Chemical composition (mass%) of the slag and MBFS

Components	MgO	Na_2O	P_2O_5	SiO_2	Al_2O_3	Fe_2O_3	MnO	TiO_2	CaO	K_2O	LOI
Slag	0.39	<0.1	0.05	49.37	34.50	2.88	0.02	0.79	5.97	0.36	5.67
MBFS	0.22	0.42	0.04	48.27	32.87	1.32	0.01	0.79	1.72	0.38	13.98

absorbance of the filtrate was measured. The dye concentration was calculated from the calibration curve. The solutions were diluted to maintain their absorbance within the linear calibration range.

The percentage removal (R, %) of the dye and the amount adsorbed q (mg/g) were calculated using the following formula:

$$R = \frac{C_0 - C_e}{C_0} \times 100 \quad (1)$$

where C_0 and C_e (mg/L) are the initial and equilibrium solution concentrations of the dyes, respectively. The adsorption amount, q_e, at the equilibrium was calculated as follows:

$$q_e = \frac{(C_0 - C_e) \times V}{m} \times 100 \quad (2)$$

where q_e is the amount of dye absorbed onto a unit dry mass of the MBFS (mg/g), V is the volume of the dye solution (L), and m is the dry weight of the hybrid materials used (g).

2.4. Effect of contact time

To study the effect of contact period and to determine the equilibrium time, batch adsorption kinetics were carried out. In this experiment, 0.05 g of the adsorbent was mixed with 25 mL each 300 mg/L dye solution. The solutions were shaken for 2, 5, 10, 30, 60, 90, and 120 min intervals and analyzed using a UV–vis spectrophotometer.

The adsorption capacities at a specific time, q_t (mg/g), were computed using Eq. (3):

$$q_t = \frac{(C_0 - C_t) \times V}{m} \quad (3)$$

where C_t represents the dyes concentration at a specific time t.

2.5. Batch kinetics studies

Lagergren pseudo-first-order, type 1 pseudo-second-order, and intraparticle diffusion models were used to study the kinetics of the adsorption of dyes on MBFS. Eqs. (4)–(6) represent pseudo-first-order and pseudo-second-order models, respectively [15,30]:

$$\log \frac{(q_e - q_t)}{q_e} = \frac{-k_1}{2.303} t \quad (4)$$

$$\frac{t}{q_t} = \frac{1}{k_2 q_e^2} + \frac{1}{q_e} t \quad (5)$$

where q_e is the calculated adsorption capacity, whereas pseudo-first-order and pseudo-second-order adsorption rate constants are represented by k_1 (min^{-1}) and k_2 (g/mg/min), respectively. The value of $q_{e,cal}$ was calculated from the intercept of the log $(q_e - q_t)$ vs. t using Eq. (4) and from the slope of t/q_t vs. t using Eq. (5):

$$q_t = k_p t^{1/2} + I \quad (6)$$

where q_t, k_p, and I are the amount of dye adsorbed (mg/g) at time t (min), intraparticle diffusion rate constant (mg/g $min^{1/2}$), and intercept, respectively.

2.6. Isotherm model studies

Isotherm study provides an insight of the association between the adsorbent's surface and dye molecules. Three well-known models, i.e. Langmuir and Freundlich models were used in this study to investigate the isothermal adsorption of dyes on MBFS. The Langmuir and Freundlich models are shown in Eqs. (7) and (8), respectively [31–33]:

$$\frac{C_e}{q_e} = \frac{1}{K_L q_m} C_e + \frac{1}{q_m} \quad (7)$$

where the adsorption capacity and energy of adsorption are represented by Langmuir constants q_m (mg/g) and K_L (L/mg), respectively, and their values can be calculated from the plot between C_e/q_e vs. C_e using Eq. (7):

$$\ln q_e = \ln K_F + \frac{1}{n} \ln C_e \quad (8)$$

where K_F and $1/n$ are the Freundlich isotherm constants, i.e. the measures of adsorption capacity and adsorption intensity, respectively. These values were calculated from the plot of $\ln(q_e)$ vs. $\ln(C_e)$ using Eq. (8). The $1/n$ values indicate that whether the type of isotherm is irreversible ($1/n = 0$), favorable ($0 < 1/n < 1$), or unfavorable ($1/n > 1$) [33].

The concentrations of AR138 and AG27 dye solutions were measured using a UV–vis spectrophotometer (Model TU-1901, Beijing Purkinje General Instrument Co. Ltd, China). The absorbance calibration curve was plotted between the absorbance and concentration of the dye solution in the concentration range 0–15 mg/L.

All the adsorption experiments were performed three times to increase the precision of the results, and only the average values were reported throughout this study.

3. Results and discussion

3.1. Physicochemical properties and characterization of adsorbent

Because the adsorption process from the liquid phase to the solid phase is influenced by the intrinsic characteristics of the adsorbent, the physicochemical

structure of slag and MBFS should be investigated for the proper interpretation of dye removal from aqueous solutions.

Table 2 shows the physical properties and main chemical compositions of the slag and MBFS. The slag contains a certain amount of metallic and nonmetallic oxide components. As shown in Table 2, the original and modified slags mainly consist of Al_2O_3 and SiO_2 (~80% by mass). A portion of LOI in the modified slag increased from 5.67% in the original slag to 13.98%, decreasing the amount of all other oxides (MgO, SiO_2, Al_2O_3, Fe_2O_3, and CaO).

Scanning electron microscopy plays an important role in characterizing the surface morphology and fundamental physical properties of the adsorbent surface. SEM is a primary tool for determining the particle shape, porosity, and appropriate size distribution of the adsorbent. Fig. 1 shows the SEM micrographs of blast-furnace slag (BFS) and MBFS. Significant differences were observed between the micrographs of the BFS before and after the modification. The SEM of BFS (Fig. 1(a) and (b)) indicates that the unmodified slag consists of many smooth surfaces and different size particles. Moreover, many pores of BFS were very small. After the modification, the smooth surface of BFS was damaged and became loose and rough due to the crushing procedure during the modification. The SEM of MBFS (Fig. 1(c) and (d)) indicates an irregular, rough, and porous surface morphology. Furthermore, many macropores were formed, thus improving the specific surface area (from 51.3 to 288.4 m^2/g) and porosity (from 48.9 to 61.6%). Moreover, the residual gap of modified slag is more beneficial to the high adsorption property of adsorbent [34]. Therefore, by modifying BFS, more and more pores were generated with an increase in the porosity volume, and the surface of the slag became coarser. These properties should facilitate the diffusion of dyes to the surface of MBFS, indicating a high adsorption rate.

3.2. Adsorption studies

3.2.1. Effect of pH and temperature on dye removal

The effect of pH was studied in the pH range 2–11 at 298 K as shown in Fig. 2(a). Fig. 3(a) shows that the removal of hazardous dyes AG27 and AR138 was almost affected by pH. The results indicate that the adsorbent facilitates dye removal in different media. Fig. 2(b) shows that the adsorption of AG27 and AR138 increased gradually with increasing temperature (from 288 to 298 K) and reached the maximum removal at 298 K. Then, the dye removal efficiency slightly decreased when the temperature was increased from 298 to 328 K. With the increase in

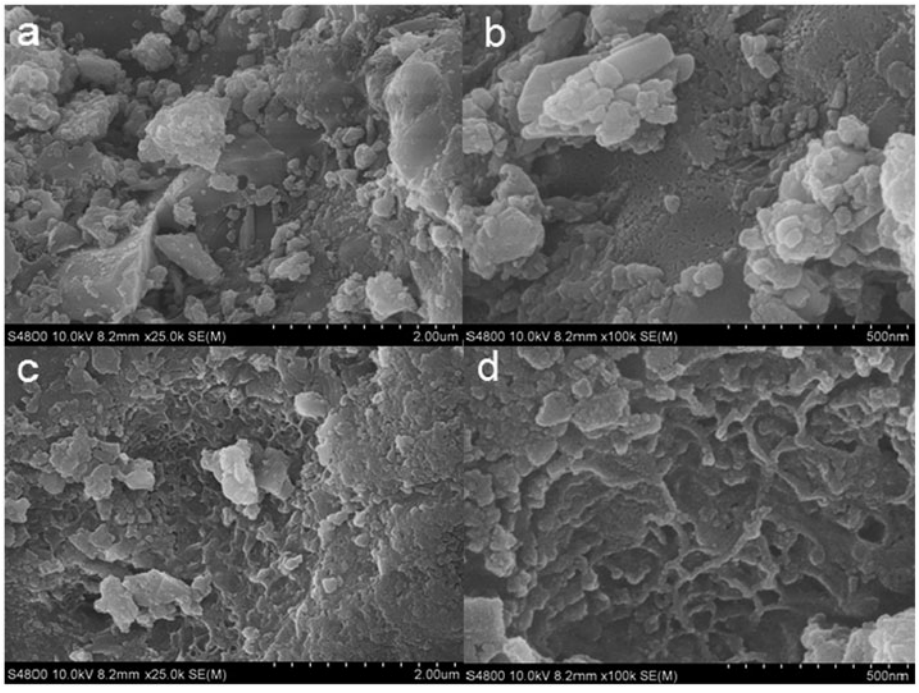

Fig. 1. SEM images of BFS (a and b) and MBFS (c and d).

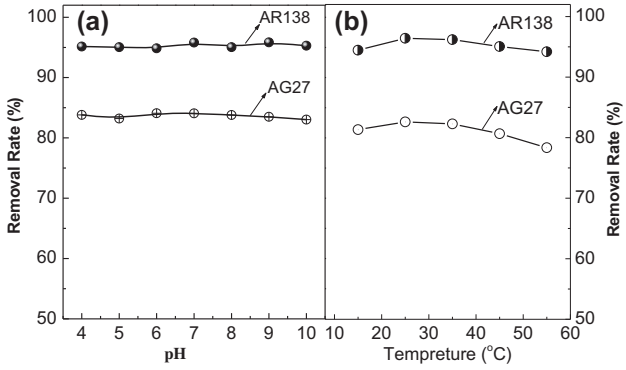

Fig. 2. Effect of pH (a) and temperature (b) for adsorption of AG27 and AR138 on MBFS (contact time: 60 min, dye concentration: 300 mg/L, adsorbent dosage: 0.02 g).

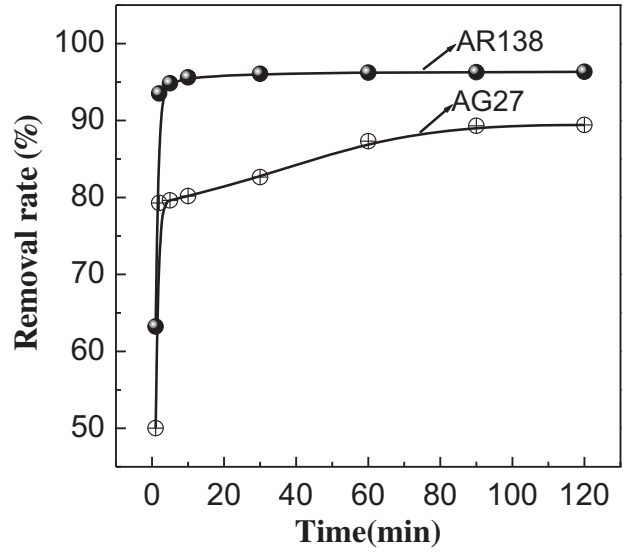

Fig. 3. Effect of contact time for adsorption of AG27 and AR138 on MBFS (dye concentration: 300 mg/L, temperature: 298 K, adsorbent dosage: 0.02 g).

temperature, the solubility of the dye also increased, the interactions between the solute and solvent became stronger than those between the solute and adsorbent. Consequently, the solute was more difficult to adsorb with further increase in temperature [35]. A similar trend has been reported for the adsorption of CR onto chitosan-coated quartz sand [36]. Furthermore, under the same experimental conditions, the maximum removal percentages of AG27 and AR138 were 96.41 and 84.61%, respectively. The results indicate that the adsorption percentage of AG27 was 12% smaller than that of AR138, indicating that AR138 had more acceptable adsorption removal. The hydrophobic property of the dodecyl group ($C_{12}H_{25}$) in the structure of AR138 is stronger than that of the butyl (C_4H_9) in the structure of AR138. This may be the probable reason for the lower adsorption abilities of AG27.

3.2.2. Effect of contact time

A good adsorbent should not only possess a large adsorption capacity, but also a fast adsorption rate. The effect of contact time was studied at room temperature for the adsorption of AG27 and AR138 on MBFS from 0 to 120 min (Fig. 3). A very rapid adsorption was observed at 10 min for both the dyes (AG27 and AR138), and a further increase in the contact time did not increase the adsorption significantly. This is because the active sites present on the MBFS surface were saturated by the dye molecules.

3.2.3. Effect of dosage on removal efficiency

To determine the effect of adsorbent dose, 60-min uptake experiments were carried out at 298 K. The results are shown in Fig. 4. The removal efficiency increased rapidly with an increase in the dosage of adsorbent, mainly because the amount of active sites increased with an increase in the amount of MBFS. When the dosage was 50 mg, the adsorption of AR138 approached equilibrium (98.21%), whereas the adsorption of AG27 approached equilibrium (97.10%) at 80 mg. However, an increase in the dosage of MBFS did not increase the removal efficiency for both AR138

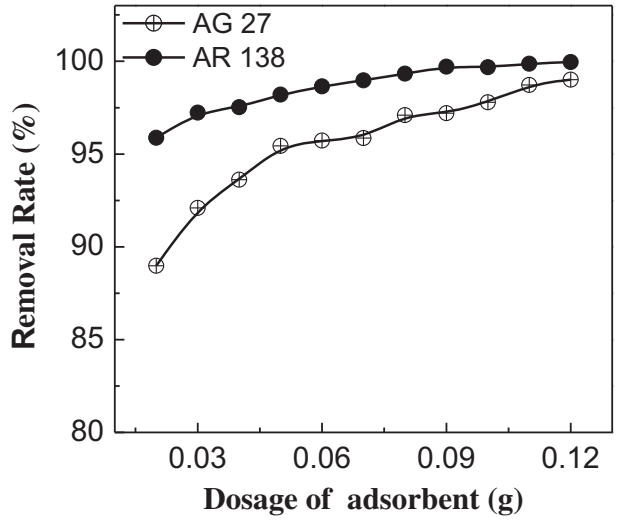

Fig. 4. Effect of dosage on adsorption behavior of AG27 and AR138 (dye concentration: 300 mg/L, volume: 10 mL, contact time: 60 min, temperature: 298 K).

and AG27 after the equilibrium. This is because the adsorption reached the saturation state, and more amount of adsorbent turned a part of the adsorption sites into waste. Considering the removal efficiency and practicality, 50 and 80 mg were selected as the optimum adsorbent dosage for AR138 and AG27, respectively, in the following studies.

3.2.4. Adsorption kinetics

Equilibrium kinetics is an important parameter for an efficient dye wastewater treatment process. To investigate the adsorption kinetics of AG27 and AR138 on MBFS and to elucidate the controlling mechanisms of adsorption process such as chemical reaction, diffusion control, and mass transfer, batch adsorption kinetics were carried out. Several kinetics models, i.e. the pseudo-first-order model, pseudo-second-order model, and the intraparticle diffusion model were used to test the experimental data [37–39]. The results are shown in Table 3. Notably, the values of R_2 for the pseudo-second-order model ($R_2 > 0.999$) were higher than those of pseudo-first-order and intraparticle diffusion models, and the calculated q_e values ($q_{e,cal}$) were closer to the experimental q_e values ($q_{e,exp}$). Thus, it can be concluded that the pseudo-second-order kinetic model is more suitable for interpreting the kinetic data in the adsorption system. Furthermore, the adsorption capacity ($q_{e,cal}$) was very close to the adsorption capacity obtained from the experimental data and pseudo-second-order model. The rate-limiting step may involve a chemical sorption between the adsorbate and adsorbent, similar to that reported in some previous reports [40–42].

3.2.5. Isotherm model studies

The distribution of the adsorbate between the sorbent and liquid phase is a measure of the position of equilibrium in the adsorption process and can be generally expressed by isotherm models. In this investigation, two different isotherm models, i.e. Langmuir and Freundlich models were applied to describe the interactions of AG27 and AR138 with MBFS.

Fig. 5(a)–(d) represents the Langmuir and Freundlich isotherm models of AG27 and AR138,

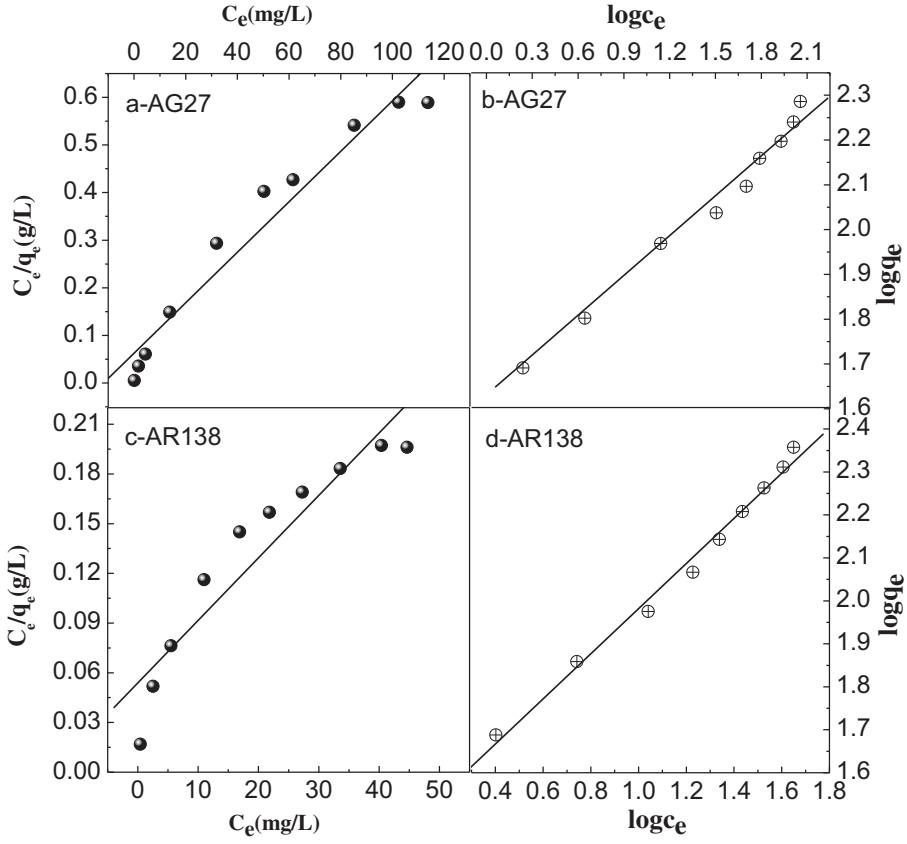

Fig. 5. Plots for Langmuir (a and c) and Freundlich (b and d) adsorption isotherms of dyes.

Table 3
Comparison of kinetics parameters for the adsorption of acid dyes on MBFS

		AG27		AR138	
		$q_{e,exp}$ (mg/g)	$t_{1/2}$ (min)	$q_{e,exp}$ (mg/g)	$t_{1/2}$ (min)
Kinetic models	Parameters	134.89	1.09	144.86	0.19
Pseudo-first-order model	$q_{e,cal}$ (mg/g)	154.89		74.13	
	k_1 (min^{-1})	0.0018		0.0019	
	R_1	0.6667		0.4172	
Pseudo-second-order model	$q_{e,cal}$ (mg/g)	134.95		144.93	
	k_2 (g/mg/min)	0.0068		0.0366	
	R_2	0.9999		1.000	
Intraparticle diffusion model	k_p (mg g/$min^{0.5}$)	0.1427		0.1118	
	I	11.88		10.16	
	R_3	0.7105		0.5014	

Table 4
Isotherm parameters for adsorption of acid dyes onto MBFS

Isotherm	Parameters	AG27	AR138
Langmuir	q_m(mg/g)	265.2	208.3
	K_L (L/mg)	0.0699	0.0538
	R_L	0.0455	0.0583
	R^2	0.8849	0.7694
Freundlich	$1/n$	0.47	0.30
	K_F	33.57	43.65
	R^2	0.9903	0.9947

respectively. Table 4 shows the isotherm parameters and the extent of fitting (R) of these isotherm models. Fig. 5(c) and (d) shows a linear plot of ln(q_e) vs. ln (C_e), indicating that the adsorption of AG27 and AR138 on MBFS follows the Freundlich isotherm. The observation was further supported by the value of R^2 (0.9903 and 0.9947 for AG27 and AR138, respectively). Table 4 shows that the extent of fitting of Langmuir models is less than the Freundlich isotherm for both the dyes, indicating that both the dyes have an approximately similar adsorption mechanism. The best fitting of the Freundlich isotherm shows that the adsorbate concentration on the adsorbent will increase with an increase in the adsorbate concentration in the solution. The $1/n$ values shown in Table 4 ($0 < 1/n < 1$) indicate that the adsorption is favored (Table 4).

3.2.6. Adsorption thermodynamics

To investigate the thermodynamic behavior of AG27 and AR138 adsorption on MBFS, parameters such as Gibbs free energy change (ΔG_0), enthalpy

Table 5
Thermodynamic parameters of dyes adsorption on MBFS (100 mL, pH 6.8, C_0 of dyes: 300 mg/L for AG27 and 400 mg/L for AR138 and MBFS: 2 g/L for AG27 and 3 g/L for AR138)

		Thermodynamic parameters		
Dyes	Temperature (℃)	ΔG_0 (kJ/mol)	ΔH_0 (kJ/mol)	ΔS_0 (J/mol/K)
AG27	15	−4.95	−34.73	−103.43
	25	−4.22		
	35	−3.84		
	45	−3.18		
AR138	15	−7.42	−14.15	−23.28
	25	−7.23		
	35	−6.93		
	45	−6.76		

(ΔH_0), and entropy (ΔS_0) were calculated using the following equations [43]:

$$K_0 = \frac{C_a}{C_e} = \frac{C_0 - C_e}{C_e} \quad (9)$$

$$\Delta G_0 = -RT \ln K_0 \quad (10)$$

$$\ln K_0 = \frac{\Delta S_0}{R} - \frac{\Delta H_0}{RT} \quad (11)$$

Table 5 shows the thermodynamic parameters for the adsorption of AG27 and AR138 at different temperatures. Negative ΔG_0 and ΔH_0 values were observed under various concentrations of dyes and temperatures, indicating that the adsorption of AG27 and AR138 onto MBFS is thermodynamically feasible, spontaneous, and exothermic. The increase in ΔG_0 values with the increase in temperature demonstrates a negative effect of temperature on adsorption. Moreover, negative ΔS_0 values indicate a reduction in the randomness at the solid–liquid interface during the adsorption [30,43]. Furthermore, the results of adsorption thermodynamics agree well with the equilibrium isotherms obtained in this study, and the optimal reaction temperature was 25°C.

4. Conclusions

In this study, the MBFS was prepared by inorganic modification using a mixture HCl and NaCl. Kinetics, equilibrium, and factors affecting dye removal were studied for the adsorption of AR138 and AG27 from aqueous solutions onto MBFS. The adsorption results show that MBFS can be effectively used as a sorbent for the removal of anionic dyes. MBFS exhibited high adsorption capacities toward AR138 and AG27. The maximum adsorption capacity was ~265.2 mg/g for AG27 and 208.3 mg/g for AR138 at 298 K. The adsorption kinetics of dyes on MBFS followed the pseudo-second-order model at different dye concentrations. The equilibrium data were analyzed. The results show that AR138 and AG27 followed the Freundlich isotherm. Based on the data obtained in this study, MBFS is an eco-friendly adsorbent for dye removal from colored textile wastewater.

Acknowledgments

This study was supported by the National Natural Science Foundation of China (Grant No. 21307015), the Science Foundation for The Excellent Youth Scholars of Higher Education of Guangdong, China (Grant No. Yq2013122), the undergraduates' scientific and technological innovation to cultivate special projects of Guangdong, China (Grant No. pdjh2015b0400), the training Programs of Innovation for Undergraduates of 2015 (Grant No. 1427815049). The authors are grateful to the projects.

References

[1] M. Muthukumar, D. Sargunamani, M. Senthilku-mar, N. Selvakumar, Studies on decolouration, toxicity and the possibility for recycling of acid dye effluents using ozone treatment, Dyes Pigm. 64 (2005) 39–44.
[2] A. Gottlieb, C. Shaw, A. Smith, A. Wheatley, S. Forsythe, The toxicity of textile reactive azo dyes after hydrolysis and decolourisation, J. Biotechnol. 101 (2003) 49–56.
[3] D. Inthorn, S. Singhtho, P. Thiravetyan, E. Khan, Decolorization of basic, direct and reactive dyes by pre-treated narrow-leaved cattail (*Typha angustifolia* Linn.), Bioresour. Technol. 94 (2004) 299–306.
[4] K.K.H. Choy, G. McKay, J.F. Porter, Sorption of acid dyes from effluents using activated carbon, Resour. Conserv. Recycl. 27 (1999) 57–71.
[5] V.K. Gupta, Application of low-cost adsorbents for dye removal—A review, J. Environ. Manage. 90 (2009) 2313–2342.
[6] T. Robinson, G. McMullan, R. Marchant, P. Niga-m, Remediation of dyes in textile effluent: A critical review on current treatment technologies with a proposed alternative, Bioresour. Technol. 77 (2001) 247–255.
[7] H.S. El-Desoky, M.M. Ghoneim, N.M. Zidan, Decolorization and degradation of Ponceau S azo-dye in aqueous solutions by the electrochemical advanced Fenton oxidation, Desalination 264 (2010) 143–150.
[8] X. Xu, H.G. Spencer, Dye-salt separations by nanofiltration using weak acid polyelectrolyte membranes, Desalination 114 (1997) 129–137.
[9] Y. Li, B. Gao, T. Wu, B. Wang, X. Li, Adsorption properties of aluminum magnesium mixed hydroxide for the model anionic dye Reactive Brilliant Red K-2BP, J. Hazard. Mater. 164 (2009) 1098–1104.
[10] K.V. Kumar, S. Sivanesan, V. Ramamurthi, Adsorption of malachite green onto *Pithophora* sp., a fresh water algae: Equilibrium and kinetic modelling, Process Biochem. 40 (2005) 2865–2872.
[11] Y.C. Sharma, Uma, Optimization of parameters for adsorption of methylene blue on a low-cost activated carbon, J. Chem. Eng. Data 55 (2010) 435–439.
[12] G. Crini, Non-conventional low-cost adsorbents for dye removal: A review, Bioresour. Technol. 97 (2006) 1061–1085.
[13] A. Demirbas, Agricultural based activated carbons for the removal of dyes from aqueous solutions: A review, J. Hazard. Mater. 167 (2009) 1–9.
[14] K.B. Tan, M. Vakili, B.A. Horri, P.E. Poh, A.Z. Abdullah, B. Salamatinia, Adsorption of dyes by nanomaterials: Recent developments and adsorption mechanisms, Sep. Purif. Technol. 150 (2015) 229–242.

[15] N.M. Mahmoodi, B. Hayati, M. Arami, C. Lan, Adsorption of textile dyes on Pine Cone from colored wastewater: Kinetic, equilibrium and thermodynamic studies, Desalination 268 (2011) 117–125.
[16] I.D. Mall, V.C. Srivastava, N.K. Agarwal, Removal of Orange-G and Methyl Violet dyes by adsorption onto bagasse fly ash: Kinetic study and equilibrium isotherm analyses, Dyes Pigm. 69 (2006) 210–223.
[17] S. Netpradit, P. Thiravetyan, S. Towprayoon, Application of waste metal hydroxide sludge for adsorption of azo reactive dyes, Water Res. 37 (2003) 763–772.
[18] Q.Q. Zhong, Q.Y. Yue, Q. Li, X. Xu, B.Y. Gao, Preparation, characterization of modified wheat residue and its utilization for the anionic dye removal, Desalination 267 (2011) 193–200.
[19] N.R. Rakhimova, R.Z. Rakhimov, Alkali-activated cements and mortars based on blast furnace slag and red clay brick waste, Mater. Des. 85 (2015) 324–331.
[20] S. Teng, T.Y. Lim, B.S. Divsholi, Durability and mechanical properties of high strength concrete incorporating ultra fine Ground granulated blast-furnace slag, Constr. Build. Mater. 40 (2013) 875–881.
[21] M.H.N. Yio, J.C. Phelan, H.S. Wong, N.R. Buenfeld, Determining the slag fraction, water/binder ratio and degree of hydration in hardened cement pastes, Cem. Concr. Res. 56 (2014) 171–181.
[22] Y. Xue, S. Wu, M. Zhou, Adsorption characterization of Cu(II) from aqueous solution onto basic oxygen furnace slag, Chem. Eng. J. 231 (2013) 355–364.
[23] C.L. Beh, T.G. Chuah, M.N. Nourouzi, T. Choong, Removal of heavy metals from steel making waste water by using electric arc furnace slag, J. Chem. 9 (2012) 2557–2564.
[24] J.M. Duan, B. Su, Removal characteristics of Cd(II) from acidic aqueous solution by modified steel-making slag, Chem. Eng. J. 246 (2014) 160–167.
[25] V.K. Jha, Y. Kameshima, A. Nakajima, K. Okada, Utilization of steel-making slag for the uptake of ammonium and phosphate ions from aqueous solution, J. Hazard. Mater. 156 (2008) 156–162.
[26] J. Yang, S. Wang, Z. Lu, J. Yang, S. Lou, Converter slag–coal cinder columns for the removal of phosphorous and other pollutants, J. Hazard. Mater. 168 (2009) 331–337.
[27] Y. Xue, H. Hou, S. Zhu, Adsorption removal of reactive dyes from aqueous solution by modified basic oxygen furnace slag: Isotherm and kinetic study, Chem. Eng. J. 147 (2009) 272–279.
[28] A. Genc, A. Oguz, Sorption of acid dyes from aqueous solution by using non-ground ash and slag, Desalination 264 (2010) 78–83.
[29] Y.J. Zhang, L.C. Liu, L.L. Ni, B.L. Wang, A facile and low-cost synthesis of granulated blast furnace slag-based cementitious material coupled with Fe_2O_3 catalyst for treatment of dye wastewater, Appl. Catal. B: Environ. 138–139 (2013) 9–16.
[30] Y.H. Wu, M.L. Zhang, H.Y. Zhao, S.G. Yang, A. Arkin, Functionalized mesoporous silica material and anionic dye adsorption: MCM-41 incorporated with amine groups for competitive adsorption of Acid Fuchsine and Acid Orange II, RSC Adv. 4 (2014) 61256–61267.
[31] Y. Kim, C. Kim, I. Choi, S. Rengaraj, J. Yi, Arsenic removal using mesoporous alumina prepared via a templating method, Environ. Sci. Technol. 38 (2004) 924–931.
[32] K.H. Goh, T.T. Lim, Z. Dong, Application of layered double hydroxides for removal of oxyanions: A review, Water Res. 42 (2008) 1343–1368.
[33] N.M. Mahmoodi, M. Arami, Modeling and sensitivity analysis of dyes adsorption onto natural adsorbent from colored textile wastewater, J. Appl. Polym. Sci. 109 (2008) 4043–4048.
[34] P.J. Xu. Study of Preparation and Property of Modified Blast Furnace Slag and It's Application [D]. Master's Thesis, Shangdong University, Jinan, 2006.
[35] A.R. Cestari, E.F.S. Vieira, A.A. Pinto, E.C.N. Lopes, Multistep adsorption of anionic dyes on silica/chitosan hybrid, J. Colloid Interface Sci. 292 (2005) 363–372.
[36] T. Feng, F. Zhang, J. Wang, L. Wang, Application of chitosan-coated quartz sand for Congo red adsorption from aqueous solution, J. Appl. Polym. Sci. 125 (2012) 1766–1772.
[37] S. Kaur, S. Rani, R.K. Mahajan, Adsorption kinetics for the removal of hazardous dye Congo Red by biowaste Materials as adsorbents, J. Chem. 2013 (2013) 1–12.
[38] K.Z. Elwakeel, Removal of Reactive Black 5 from aqueous solutions using magnetic chitosan resins, J. Hazard. Mater. 167 (2009) 383–392.
[39] N. Hoda, E. Bayram, E. Ayranci, Kinetic and equilibrium studies on the removal of acid dyes from aqueous solutions by adsorption onto activated carbon cloth, J. Hazard. Mater. 137 (2006) 344–351.
[40] M.S. Sajab, C.H. Chia, S. Zakaria, P.S. Khiew, Cationic and anionic modifications of oil palm empty fruit bunch fibers for the removal of dyes from aqueous solutions, Bioresour. Technol. 128 (2013) 571–577.
[41] S. Dawood, T.K. Sen, Removal of anionic dye Congo red from aqueous solution by raw pine and acid-treated pine cone powder as adsorbent: Equilibrium, thermodynamic, kinetics, mechanism and process design, Water Res. 46 (2012) 1933–1946.
[42] Y. Feng, D.D. Dionysiou, Y. Wu, H. Zhou, L. Xue, S. He, L. Yang, Adsorption of dyestuff from aqueous solutions through oxalic acid-modified swede rape straw: Adsorption process and disposal methodology of depleted bioadsorbents, Bioresour. Technol. 138 (2013) 191–197.
[43] M. Jain, V. Garg, K. Kadirvelu, Chromium(VI) removal from aqueous system using *Helianthus annuus* (sunflower) stem waste, J. Hazard. Mater. 162 (2009) 365–372.